European Conference on Computational Fluid Dynamics
ECCOMAS CFD 2006
P. Wesseling, E. Oñate and J. Périaux (Eds)

MULTISCALE METHODS IN COMPUTATIONAL FLUID AND SOLID MECHANICS

René de Borst[*,†], Steven J. Hulshoff[*], Stefan Lenz[‡], Edwin A. Munts[*], Harald van Brummelen[*] and Wolfgang A. Wall[‡]

[*]Delft University of Technology, Faculty of Aerospace Engineering
Kluyverweg 1, 2629 HS, The Netherlands
e-mail: r.deborst,s.j.hulshoff,e.a.munts,e.h.vanbrummelen@tudelft.nl
web page: http://www.em.lr.tudelft.nl
[†]LaMCoS CNRS-UMR 5514, INSA de Lyon, 69621 Villeurbanne, France
[‡]Technische Universität München, Lehrstuhl für Numerische Mechanik,
Garching, Germany
e-mail: lenz,wall@lnm.tum.de

Key words: multiscale methods, fluid flow, turbulence, fluid-structure interaction, multigrid methods

Abstract. *First, an attempt is made towards gaining a more systematic understanding of recent progress in multiscale modelling in computational solid and fluid mechanics. Subsequently, the discussion is focused on variational multiscale methods for the compressible and incompressible Navier-Stokes equations. Examples are given of the application of this class of methods to a turbulent channel flow. Finally, multigrid methods, which can also be conceived as a subclass of multiscale methods, are applied to fluid-structure interaction problems.*

1 INTRODUCTION

The basic idea of multiscale methods, namely the decomposition of a problem into a coarse scale and a fine scale, has in an intuitive manner been used in engineering for many decades, if not for centuries. Also in computational science, large-scale problems have been solved, and local data, for instance displacements, forces or velocities, have been used as boundary conditions for the resolution of more detail in a part of the problem. Recent years have witnessed the development of multiscale methods in computational science, which strive at coupling fine scales and coarse scales in a more systematic manner. Having made a rigorous decomposition of the problem into fine scales and coarse scales, various approaches exist, which essentially only differ in how to couple the fine scales to the coarse scale. The Variational Multiscale Method proposed by Hughes and co-workers[1–4] is a most promising member of this family, but for instance, multigrid methods can also be classified as multiscale methods. The same conjecture can be substantiated for

hp-adaptive methods. In this contribution we will give a succinct taxonomy of various multiscale methods.

Next, we will briefly review the Variational Multiscale Method and we will discuss VMM formulations for the compressible and the incompressible Navier-Stokes equations. The formulation for compressible flow uses a spatial discretisation corresponding to a high-order continuous Galerkin method, which due to its hierarchical nature provides a natural framework for 'a priori' scale separation. The latter property is crucial. The method is formulated to support both continuous and discontinuous discretisations in time. The formulation for incompressible flow uses an approach where only resolved and subgrid scales are distinguished, the latter being approximated analytically. Results will be presented from both formulations applied to turbulent channel flow.

Finally, multigrid methods will be applied to fluid-structure interaction problems. The basic iterative method for fluid-structure interaction problems employs defect correction. The latter provides a suitable smoother for a multigrid process, although in itself the associated subiteration process converges slowly. Indeed, the smoothed error can be represented accurately on a coarse mesh, which results in an effective coarse-grid correction. It is noted that an efficient solution strategy is made possible by virtue of the relative compactness of the displacement-to-pressure operator in the fluid-structure interaction problem. This relative compactness manifests the difference in length and time scales in the fluid and the structure and, in this sense, the multigrid method exploits the inherent multiscale character of fluid-structure-interaction problems.

2 A TAXONOMY OF MULTISCALE METHODS

Multiscale methods have seen a tremendous development during the past years. Nevertheless, only a limited number of attempts appear to have been made to review and classify the various approaches. Notable exceptions are Brandt[5], who focuses on solver technologies, and Engquist[6], who have developed a heterogeneous multiscale method as a general framework. According to Bochev *et al.*[7] the variational multiscale method introduced by Hughes and co-workers[1–4] can serve as a general framework for multiscale methods. A more specific overview on variational multiscale method for laminar and turbulent flows from has been presented by Gravemeier *et al.*[8]. In view of the above, it was considered to be timely to develop a taxonomy for multiscale approaches, displaying the necessary building blocks which are used for different applications and from sometimes very different view points. Before investigating the different classification aspects in more detail, however, we will briefly discuss some examples of multiscale methods in computational solid and fluid mechanics.

In the Discontinuous Enrichment Method[9], the finite element method is enriched with homogeneous free-space solutions, which represent the fine scales. Using a Lagrange multiplier technique, the fine-scale solutions are then weakly coupled to the large scales. For laminar and turbulent flows two-level and three-level variational multiscale methods[10–12] are rapidly gaining popularity, as well as a newer variant of the variational

multiscale method, the so-called New Variational Multiscale Method[13]. In the first applications of variational multiscale methods, the fine scales are represented by residual-free bubbles[10–12], whereas in the latter approach[13] analytical expressions are used to account for the influence of the fine scales on the large scales. It is emphasised that variational multiscale methods can be used in conjunction with various discretisation method methods, for instance, finite element or finite volume methods.

There are four features in multiscale methods which are crucial for the distinction between the different approaches: (i) the properties of the underlying physical problem, (ii) the processing with respect to the spatial scale, (iii) the processing with respect to the temporal scale, and (iv) the properties of the solver. Below we will discuss them in greater detail.

Properties of the underlying problem. The underlying problem can be classified by questions like: is it a problem described by different equations on different scales or may one equation describe all relevant scales, how many scale levels have to be considered, how strong is the coupling between the scales, is there a periodic microscale structure, and is the fine scale information required locally or globally?

An example of a problem where the same set of equations describe the different scales is turbulence. Indeed, the Navier-Stokes equations are able to capture all relevant scales of Newtonian fluid flow, including the turbulent flow regime. On the other hand, Molecular Dynamics approaches utilise very different equations than those used by finite element methods for continua, and multiscale methods for coupling them, e.g. the Bridging Domain Method[14], have a different character. Indeed, when, as in the latter case, such different descriptions are used on both scales, one may be tempted to call this a multiphysics problem, although in a strict sense it is not.

The question of how many scale levels have to be considered is often constrained by the available computer power. So far, most problems are treated by a two-level approach, whereas in turbulence simulations we encounter three-level approaches as well. In contrast to, e.g., crack propagation in solids and structures, where the fine scale information is required only locally, global fine-scale information is necessary in turbulent flows.

Spatial scale processing. The various approaches that address the processing of the spatial scales can be distinguished by considering the following aspects: What kind of discretisation is applied (coarse to fine, fine to coarse, or separate domains), how are the fine scales represented, how is the inter-element continuity on the fine-scale and on the large-scale levels taken care of, which are the assumptions on the boundaries of the fine-scales, how is information passed between the scales?

Concerning the discretisation, the coarse-to-fine-approach departs from a large-scale discretisation. The fine-scale information is evaluated either locally or globally in this case. The Discontinuous Enrichment Method is believed to belong to this class. On the other hand, the fine-to-coarse approach departs from a fine-scale discretisation from which the large-scale representation is derived, e.g., in multigrid approaches like Discrete-to-Continuum Bridging[15], which has been used to couple fine-scale molecular dynamics

<table>
<tr><th colspan="8">Spatial scale processing</th></tr>
<tr><td rowspan="2" colspan="2">Discretization methodology</td><td colspan="2">Coarse to fine approach</td><td colspan="2">Fine to coarse approach</td><td colspan="2">Separate domains</td></tr>
<tr><td>Only local microscale evaluation</td><td>Microscale evaluation everywhere</td><td colspan="2">Microscale evaluation everywhere</td><td colspan="2">Only local microscale evaluation</td></tr>
<tr><td rowspan="3" colspan="2">(Fine-)Scale representation</td><td colspan="2">2 scales</td><td colspan="2">2 scales or more</td><td colspan="2">More than 2 scales</td></tr>
<tr><td>Residual-free bubbles</td><td>Stabilization term</td><td>Agglomeration</td><td>Molecules (MD)</td><td colspan="2">Viscosity (3LFEM)</td></tr>
<tr><td colspan="2">Homogeneous free-space solutions (DEM)</td><td>h/p-refinement</td><td>Stabilization term</td><td colspan="2"></td></tr>
<tr><td rowspan="2">Interelemental continuity</td><td>Large scale</td><td colspan="3">Continuous</td><td colspan="3">Discontinuous</td></tr>
<tr><td>Small scale</td><td>Continuous</td><td colspan="2">Discontinuous</td><td colspan="4">Algebraic operators approx. local Green's fctn</td></tr>
<tr><td rowspan="2" colspan="2">Microscale boundary conditions</td><td rowspan="2">No assumptions (DGM, DEM)</td><td colspan="6">assumptions</td></tr>
<tr><td colspan="2">Homogeneous Dirichlet BC</td><td>Nodal values zero</td><td colspan="2">Periodic microscale structure</td><td>Linear interpolation of Hamiltonians</td></tr>
<tr><td colspan="2">Interscale communication</td><td>Variational projection</td><td colspan="2">Lagrange multiplier method</td><td colspan="2">Prolongation/ restriction</td><td>Node-to-node-coupling</td></tr>
</table>

Figure 1: Matrix that classifies spatial processing aspects of multiscale methods

to large-scale continuum mechanics.

On the large-scale level, most methods assume continuity between the individual elements, whereas on the small-scale level, for instance, the molecular dynamics approaches are discontinuous. If the physical problem allows for assumptions on the small-scale level, computationally efficient procedures may be developed, such as in the two-level and three-level variational multiscale methods. Also for the communication between the scales – a most essential part of multiscale methods, a wide variety of possibilities exists, ranging from variational projection as in the New Variational Multiscale Method, to Lagrange multiplier methods as utilised in the Discontinuous Enrichment Method. Figure 1 attempts to classify the various aspects that relate to spatial processing.

Temporal scale processing. With respect to the processing of the temporal scales, we distinguish between so-called concurrent, two-way coupled procedures and sequential, or serial procedures. In the latter case, at a given moment in time, the fine scales and the large scales can be treated independently, which contrasts with the first case. Another aspect is the space-time coupling: is one framework used for the spatial dimensions as well as for the time, or are they treated differently? Most methods discretise space and time in different ways, a notable exception being the space-time finite element method. One can further distinguish between methods which use the same time step on all scales and methods that use subcycling, as, e.g., is done in the Bridging Domain Method[14]. The matrix of Figure 2 attempts to display the relevant aspects of the processing of the temporal scale.

Properties of the solver. Since all numerical methods, including multiscale methods,

<table>
<tr><th colspan="5">Temporal scale processing</th></tr>
<tr><td>Temporal scale coupling</td><td>Concurrent, two-way coupled</td><td colspan="3">Sequential, serial</td></tr>
<tr><td rowspan="3">Space-time coupling</td><td>One framework</td><td colspan="3">Different frameworks</td></tr>
<tr><td rowspan="2">Space-time FEM</td><td>Runge-Kutta</td><td>One-step-theta</td><td rowspan="2">Verlet</td></tr>
<tr><td>Central difference</td><td>Newmark</td></tr>
<tr><td>Time-step-size</td><td>Same time step</td><td colspan="3">Subcycling:
Assumption of constant macrostep acceleration allows macroscale interpolation at every microstep</td></tr>
</table>

Figure 2: Matrix that classifies temporal processing aspects of multiscale methods

in the end require a linear system of equations to be solved, the connection of the solver to the multiscale method is an important issue. Normally, the solver is not engaged in the multiscale decomposition, although there are exceptions like Discrete-to-Continuum Bridging. In this context the question arises whether the procedure is easy to parallellise.

The thoughts sketched above, preliminary as they are, can perhaps be considered as a prototype scheme to compare various methods. This can help in the assessment of different methods and to obtain a clearer view on differences and similarities between (seemingly) different approaches. The structure may also allow for the identification of a more general framework which is applicable to various fields of interest.

3 MULTISCALE METHODS FOR FLUID FLOW

Turbulence is characterised by a continuous range of scales which is normally too broad to allow direct computation. In practice, however, it is often only the dynamics of the largest scales which are of direct interest. In order to accurately compute their behaviour, one must reproduce their interactions with smaller scales of comparable size. These interactions are typically inviscid in nature, although their net effect is to transfer kinetic energy to smaller scales.

Conventional techniques for large-eddy simulation of turbulent flows normally consider a range of scales beyond those of interest, so that interactions with smaller scales are adequately represented. To limit the distortion of small resolved scales by the absence of interactions with unresolved scales, a dissipative model is normally added to the governing equations. Such models remove energy from all resolved scales in order to account for the energy transfer from the small resolved scales to the unresolved scale range.

Hughes[3] pointed out that the variational multiscale method, originally developed to provide a framework for subgrid-scale modelling and stabilisation, could be used to project the unresolved-scale model onto the dynamics of the smaller resolved scales alone. Initial implementations[4] made use of global spectral discretisations in order to unambiguously

separate the large and small resolved scales. Later, Jansen[16] and Collis[17] used finite-element discretisations where scale separation was performed using a hierarchical basis. Collis noted that Hughes' original method could be interpreted as a three-level multiscale method with different modelling assumptions for the large resolved, small resolved and unresolved scales. An alternative form of scale separation has been pursued by Koobus and Farhat[18] who constructed larger resolved scales on unstructured meshes via element agglomeration.

3.1 The three-level variational multiscale method

In this subsection we describe a three-level variational multiscale discretisation for the compressible Navier-Stokes equations using space-time finite elements. Although explicit time-integration methods are usually used for large-eddy simulation, implicit space-time formulations are advantageous in that they allow the time step to be chosen based on large-scale accuracy requirements rather than by stability restrictions imposed by the small resolved scales.

The compressible Navier-Stokes equations in conservation form can be written as

$$\mathbf{U}_{,t} + \mathbf{F}_{i,i}(\mathbf{U}) - \mathbf{F}^v_{i,i}(\mathbf{U}) = \mathbf{S}, \tag{1}$$

where $\mathbf{U} = \{\rho, \rho\mathbf{u}, \rho e\}^T$ is the vector of conservative variables, ρ the fluid density, $\mathbf{u} = \{u, v, w\}^T$ the fluid velocity vector, e is the total energy per unit mass, $\mathbf{F}_i(\mathbf{U})$ are the non-linear inviscid fluxes, $\mathbf{F}^v_i(\mathbf{U})$ are the viscous fluxes and $\mathbf{S}$ is the source vector. Differentiation is implied with respect to variables after the comma. Introducing a trial space $\mathcal{Y}_n$ and a test space $\mathcal{W}_n$, the variational formulation can then be stated as follows: *Find* $\mathbf{Y} \in \mathcal{Y}_n$ *such that* $\forall\ \mathbf{W} \in \mathcal{W}_n$

$$\begin{aligned} -\left(\mathbf{W}_{,t}, \mathbf{U}(\mathbf{Y})\right)_{Q_n} - \left(\mathbf{W}_{,i}, \mathbf{F}_i(\mathbf{Y}) - \widetilde{\mathbf{K}}_{ij}\mathbf{Y}_{,j}\right)_{Q_n} \\ + \left(\mathbf{W}, \left(\mathbf{F}_i(\mathbf{Y}) - \mathbf{F}^v_i(\mathbf{Y})\right) n_i\right)_{P_n} + \left(\mathbf{W}(t_{n+1}), \mathbf{U}(\mathbf{Y}(t_{n+1}))\right)_{\Omega_{n+1}} \\ - \left(\mathbf{W}(t_n), \mathbf{U}(\mathbf{Y}(t_n))\right)_{\Omega_n} = \left(\mathbf{W}, \mathbf{S}\right)_{Q_n}. \end{aligned} \tag{2}$$

Here $(,)_{\Omega_n}$ denotes the L_2-inner product over region Ω_n, Ω_n is the spatial domain at time t_n, Q_n is the portion of space-time domain between time levels t_n and t_{n+1}, and P_n is the surface connecting the boundary of Ω_n with that of Ω_{n+1}. n_i is the local space-time surface normal vector. The viscous fluxes are expressed using diffusivity matrices $\widetilde{\mathbf{K}}_{ij}$ such that $\mathbf{F}^v_i(\mathbf{U}) = (\widetilde{\mathbf{K}}_{ij}\mathbf{Y}_{,j})_{,i}$. Equation (2) can be expressed compactly as:

$$B(\mathbf{W}, \mathbf{U}) = (\mathbf{W}, \mathbf{S}). \tag{3}$$

To construct a variational multiscale method, a three-level decomposition of the trial and test space is performed:

$$\mathbf{U} = \overline{\mathbf{U}} + \widetilde{\mathbf{U}} + \widehat{\mathbf{U}}, \qquad \mathbf{W} = \overline{\mathbf{W}} + \widetilde{\mathbf{W}} + \widehat{\mathbf{W}}, \tag{4}$$

where the bar denotes the large resolved scales, the tilde denotes the small resolved scales and the hat denotes the unresolved scales. To facilitate the separation of large and small resolved scales, a hierarchical basis of Legendre polynomials is employed within each element, see Munts[19] for details. The equations for the resolved scale ranges are then

$$\text{Large:} \quad B(\overline{\mathbf{W}}, \overline{\mathbf{U}} + \widetilde{\mathbf{U}} + \widehat{\mathbf{U}}) = (\overline{\mathbf{W}}, \mathbf{S}) \tag{5}$$

$$\text{Small:} \quad B(\widetilde{\mathbf{W}}, \overline{\mathbf{U}} + \widetilde{\mathbf{U}} + \widehat{\mathbf{U}}) = (\widetilde{\mathbf{W}}, \mathbf{S}) \tag{6}$$

where for example, the large-scale equation can be expanded as:

$$\begin{aligned} B(\overline{\mathbf{W}}, \overline{\mathbf{U}}) + B'(\overline{\mathbf{W}}, \overline{\mathbf{U}}, \widetilde{\mathbf{U}}) - R(\overline{\mathbf{W}}, \widetilde{\mathbf{U}}) = (\overline{\mathbf{W}}, \mathbf{S}) \\ - B'(\overline{\mathbf{W}}, \overline{\mathbf{U}}, \widehat{\mathbf{U}}) + R(\overline{\mathbf{W}}, \widehat{\mathbf{U}}) + C(\overline{\mathbf{W}}, \widetilde{\mathbf{U}}, \widehat{\mathbf{U}}), \end{aligned} \tag{7}$$

where $B'(\overline{\mathbf{W}}, \overline{\mathbf{U}}, \mathbf{U}')$ is the operator $B(\overline{\mathbf{W}}, \overline{\mathbf{U}})$ linearised about $\overline{\mathbf{U}}$ for a linear perturbation $\mathbf{U}'$, and $C(\overline{\mathbf{W}}, \widetilde{\mathbf{U}}, \widehat{\mathbf{U}})$ and $R(\overline{\mathbf{W}}, \widetilde{\mathbf{U}})$ are generalised cross and Reynolds stress projections onto the large scales.

It is assumed that interactions only occur between scales of like size, so that the unresolved scale terms in the large-scale equation can be neglected. Furthermore, it is assumed that the terms involving unresolved scales in the small-scale equation can be replaced by a single model term. This results in:

$$B(\overline{\mathbf{W}}, \overline{\mathbf{U}}) + B'(\overline{\mathbf{W}}, \overline{\mathbf{U}}, \widetilde{\mathbf{U}}) - R(\overline{\mathbf{W}}, \widetilde{\mathbf{U}}) = (\overline{\mathbf{W}}, \mathbf{S}) \tag{8}$$

$$B'(\widetilde{\mathbf{W}}, \overline{\mathbf{U}}, \widetilde{\mathbf{U}}) - R(\widetilde{\mathbf{W}}, \widetilde{\mathbf{U}}) = -[B(\widetilde{\mathbf{W}}, \overline{\mathbf{U}}) - (\widetilde{\mathbf{W}}, \mathbf{S})] + \mathbf{M}(\widetilde{\mathbf{W}}, \widetilde{\mathbf{U}}) \tag{9}$$

A simple constant-coefficient Smagorinsky model is used for $\mathbf{M}(\widetilde{\mathbf{W}}, \widetilde{\mathbf{U}})$. As this term is projected only onto the small resolved scales, the magnitude of the Smagorinsky coefficient must be increased beyond its standard value so that the amount of kinetic energy removed from the system matches that normally removed by the unresolved scales. The scaling of the coefficient is performed using the arguments of Lilly[3,20].

By restricting the direct effects of the model to the small resolved scales, the three-level method described above addresses the incongruency of applying a purely dissipative model to the large scales of interest, whose dynamics are in reality dominated by inviscid processes. In common with conventional large-eddy simulation techniques, however, the three-level approach still requires a sacrificial range of small resolved scales, whose detailed behaviour is not of direct interest, but whose computation requires significant effort. Alternatively, the variational multiscale method can be used as a framework for developing models which more accurately represent the true interactions of the unresolved scales, with the objective of eliminating the need for a wide range of sacrificial scales. This is the approach pursued in the next section.

3.2 The residual-based variational multiscale method

In the three-level approaches, the subgrid scales are modelled by a subgrid viscosity approach. Recently, Calo[13] proposed a two-level approach for incompressible flow, where only resolved and subgrid scales are distinguished. The subgrid scales are approximated analytically based on experience with stabilised methods. In this procedure, no additional artificial subgrid viscosity is introduced.

In conservative form the incompressible Navier-Stokes equations are given as

$$\begin{aligned} \mathcal{L}_m(\mathbf{u},p) &= \mathbf{u}_{,t} + \nabla\cdot(\mathbf{u}\otimes\mathbf{u}) - 2\nu\nabla\cdot\varepsilon(\mathbf{u}) + \nabla p = \mathbf{f} \\ \mathcal{L}_c(\mathbf{u}) &= \nabla\cdot\mathbf{u} = 0. \end{aligned} \tag{10}$$

where p is the kinematic pressure, $\varepsilon(\mathbf{u})$ the rate of velocity tensor, ν the kinematic viscosity and $\mathbf{f}$ a volume force. $\mathcal{L}_m(\mathbf{u},p)$ and $\mathcal{L}_c(\mathbf{u})$ represent the differential operators for the momentum and the continuity equations, respectively.

For the variational formulation, trial and test function spaces are introduced, $\mathcal{V}$ and $\mathcal{W}$, respectively. A variational formulation of Eq. (10) amounts to finding: $\mathbf{u}, p \in \mathcal{V}$ such that

$$\begin{aligned} (\mathbf{w}, \mathcal{L}_m(\mathbf{u},p)) &= (\mathbf{w},\mathbf{f}) \\ (q, \mathcal{L}_c(\mathbf{u})) &= 0 \qquad\qquad \forall \mathbf{w}, q \in \mathcal{W} \end{aligned} \tag{11}$$

In the variational multiscale framework, the trial and the test function spaces are decomposed as a direct sum of the function spaces, namely into resolved $(...)^h$ and subgrid $\hat{(...)}$ scales. Both the large and the unresolved scale equations contain purely large scale, purely fine scale, and mixed scale components:

$$\begin{aligned} (\mathbf{w}^h, \mathcal{L}_m(\mathbf{u},p)) &= (\mathbf{w}^h, \mathcal{L}_m(\mathbf{u}^h,p^h)) + (\mathbf{w}^h, \mathcal{L}_m(\hat{\mathbf{u}},\hat{p})) + (\mathbf{w}^h, \nabla\cdot(\mathbf{u}^h\otimes\hat{\mathbf{u}} + \hat{\mathbf{u}}\otimes\mathbf{u}^h)) = (\mathbf{w}^h,\mathbf{f}) \\ (q^h, \mathcal{L}_c\mathbf{u}) &= (q^h, \mathcal{L}_c\mathbf{u}^h) + (q^h, \mathcal{L}_c\hat{\mathbf{u}}) = 0 \end{aligned} \tag{12}$$

$$\begin{aligned} (\hat{\mathbf{w}}, \mathcal{L}_m(\mathbf{u},p)) &= (\hat{\mathbf{w}}, \mathcal{L}_m(\mathbf{u}^h,p^h)) + (\hat{\mathbf{w}}, \mathcal{L}_m(\hat{\mathbf{u}},\hat{p})) + (\hat{\mathbf{w}}, \nabla\cdot(\mathbf{u}^h\otimes\hat{\mathbf{u}} + \hat{\mathbf{u}}\otimes\mathbf{u}^h)) = (\hat{\mathbf{w}},\mathbf{f}) \\ (\hat{q}, \mathcal{L}_c\mathbf{u}) &= (\hat{q}, \mathcal{L}_c\mathbf{u}^h) + (\hat{q}, \mathcal{L}_c\hat{\mathbf{u}}) = 0. \end{aligned} \tag{13}$$

The idea behind this approach is that the subgrid scales contain all effects which are not captured by the chosen discretisation. In large-eddy simulations of turbulent flow using a finite element discretisation, this includes the *physical* turbulent subgrid scales as well as *numerical* phenomena.

The idea of the residual-based variational multiscale large-eddy simulations is to use the set of subgrid scale equations in order to approximate the subgrid scale velocity $\hat{\mathbf{u}}$ and the pressure $\hat{p}$, i.e. the set of subgrid scale equations is actually not discretised and solved for. Analytical approximations are derived instead, based on experience with stabilised methods. By inserting these approximations for the subgrid scale fields in the set of large resolved scale equations, a solution for the desired quantities $\mathbf{u}^h$ and p^h is found.

The momentum part of the exact subgrid scale equations, Eq. (13), can be rewritten as

$$(\hat{\mathbf{w}}, \hat{\mathbf{u}}_{,t} + \nabla\cdot ((\mathbf{u}^h \otimes \hat{\mathbf{u}}) + (\hat{\mathbf{u}} \otimes \mathbf{u}^h) + (\hat{\mathbf{u}} \otimes \hat{\mathbf{u}})) - 2\nu\nabla\cdot \varepsilon(\hat{\mathbf{u}}) + \nabla\hat{p} + \mathbf{r}_m^h) = 0, \tag{14}$$

where $\mathbf{r}_m^h$ denotes the large scale residual

$$\mathbf{r}_m^h \;=\; \mathbf{u}^h{}_{,t} + \nabla\cdot (\mathbf{u}^h \otimes \mathbf{u}^h) - 2\nu\nabla\cdot \varepsilon(\mathbf{u}^h) + \nabla p^h - \mathbf{f}. \tag{15}$$

Calo[13] has shown different possibilities for analytical approximations for Eq. (14). The simplest is to neglect the nonlinear terms $\nabla \cdot (\mathbf{u}^h \otimes \hat{\mathbf{u}})$ and $\nabla \cdot (\hat{\mathbf{u}} \otimes \hat{\mathbf{u}})$. Moreover, it is assumed, that the subgrid scale pressure $\nabla\hat{p}$ is independent of the subgrid scale momentum equation, i.e. it is exclusively determined by the subgrid scale continuity equation. It is recalled that these assumptions only concern the subgrid scale equation. This limits the influence of these assumptions on the large resolved scale in which we are interested.

Eq. (14) may be rewritten using the assumptions mentioned above

$$(\hat{\mathbf{w}}, \mathcal{L}_{\mathbf{u}^h}\hat{\mathbf{u}} + \mathbf{r}_m^h) = 0. \tag{16}$$

where the differential operator $\mathcal{L}_{\mathbf{u}^h}\mathbf{x} = \mathbf{x}_{,t} + \nabla\cdot (\mathbf{x} \otimes \mathbf{u}^h) - 2\nu\nabla\cdot \varepsilon(\mathbf{x})$ is introduced. Using a fine scale Green's function $\hat{\mathbf{g}}(\mathbf{x}, \mathbf{y})$ for the adjoint operator $\mathcal{L}^*_{\mathbf{u}^h}$, Eq. (16) can be solved for $\hat{\mathbf{u}}$.

$$\hat{\mathbf{u}}(\mathbf{y}) \;=\; -(\hat{\mathbf{g}}(\mathbf{x}, \mathbf{y}), \mathbf{r}_m^h(\mathbf{x}))_{\Omega_x} \tag{17}$$

As a result, the subgrid scale velocity is approximated by the negative inner product of the subgrid scale Green's function and the large scale residual. Unfortunately, there exists no analytical expression for the subgrid scale Green's function for the general case. Some recent findings have been presented by Hughes and Sangalli[21].

A well established approach[1,2] is to introduce local, i.e. element Green's functions $\hat{\mathbf{g}}_e(\mathbf{x}, \mathbf{y})$ as an approximation. In this case, homogeneous Dirichlet boundary conditions are assumed at element boundaries which means that the mutual influence of the subgrid velocities is confined to individual elements.

The element mean value of the element Green's function is what the stabilisation parameter τ_m, commonly used to stabilise the Navier-Stokes equations, approximates. Thus, the integral operator $\int_{\Omega_x} \hat{\mathbf{g}}_e(\mathbf{x}, \mathbf{y})$ is approximated by the algebraic operator τ_m, turning Eq. (17) into

$$\hat{\mathbf{u}} = -\tau_m \mathbf{r}_m^h \tag{18}$$

The analytical approximation for the subgrid-scale velocity can now be inserted in the large scale equations. Following the principles of stabilised methods the subgrid scale pressure is approximated by

$$\hat{p} = -\tau_c r_c^h = -\tau_c \nabla\cdot u^h \tag{19}$$

Eq. (12) contains purely large scale parts. After integration by parts, they can be identified as the common Galerkin terms:

$$\begin{aligned}(\mathbf{w}^h, \mathcal{L}_m(\mathbf{u}^h, p^h)) + \ldots &= (\mathbf{w}^h, \mathbf{f}) \\ (\mathbf{w}^h, \mathbf{u}^h_{,t}) - (\nabla \mathbf{w}^h, \mathbf{u}^h \otimes \mathbf{u}^h)) + 2\nu(\varepsilon(\mathbf{w}^h), \varepsilon(\mathbf{u}^h)) - (\nabla\cdot \mathbf{w}^h, p) + \ldots &= (\mathbf{w}^h, \mathbf{f}) \quad (20)\end{aligned}$$

$$\begin{aligned}(q^h, \mathcal{L}_c(\mathbf{u}^h)) + \ldots &= 0 \\ (q^h, \nabla\cdot \mathbf{u}^h) + \ldots &= 0. \quad (21)\end{aligned}$$

Integration by parts yields for the subgrid scale terms of Eq. (12):

$$\begin{aligned}\ldots + (\mathbf{w}^h, \mathcal{L}_m(\hat{\mathbf{u}}, \hat{p})) + (\mathbf{w}^h, \nabla\cdot (\mathbf{u}^h \otimes \hat{\mathbf{u}} + \hat{\mathbf{u}} \otimes \mathbf{u}^h)) &= \ldots \\ \ldots + (\mathbf{w}^h, \hat{\mathbf{u}}_{,t}) - 2\nu(\nabla\cdot \varepsilon(\mathbf{w}^h), \hat{\mathbf{u}}) - (\nabla \mathbf{w}^h, \mathbf{u}^h \otimes \hat{\mathbf{u}} + \hat{\mathbf{u}} \otimes \mathbf{u}^h + \hat{\mathbf{u}} \otimes \hat{\mathbf{u}}) - (\nabla\cdot \mathbf{w}^h, \hat{p}) &= (22)\end{aligned}$$

$$\begin{aligned}\ldots + (q^h, \mathcal{L}_c\hat{\mathbf{u}}) &= \ldots \\ \ldots - (\nabla q^h, \hat{\mathbf{u}}) &= \ldots \quad (23)\end{aligned}$$

The only term which is subsequently neglected in the large scale equations is the time derivative of the subgrid scale velocity, which amounts to assuming quasi-static subgrid scales. Inserting the approximations for the subgrid scale, Eqs (18) and (19), gives for the subgrid scale terms of Eqs (22) and (23)

$$\begin{aligned}&2\nu(\nabla\cdot \varepsilon(\mathbf{w}^h), \tau_m \mathbf{r}^h_m) + (\nabla \mathbf{w}^h, \mathbf{u}^h \otimes \tau_m \mathbf{r}^h_m + \tau_m \mathbf{r}^h_m \otimes \mathbf{u}^h - \tau_m \mathbf{r}^h_m \otimes \tau_m \mathbf{r}^h_m) + (\nabla\cdot \mathbf{w}^h, \tau_c \nabla\cdot \mathbf{u}^h) \\ &\underline{2\nu(\nabla\cdot \varepsilon(\mathbf{w}^h), \tau_m \mathbf{r}^h_m)} + (\tau_m \mathbf{r}^h_m \nabla \mathbf{w}^h, \mathbf{u}^h) + \underline{(\mathbf{u}^h \nabla \mathbf{w}^h, \tau_m \mathbf{r}^h_m)} - (\tau^2_m \mathbf{r}^h_m \nabla \mathbf{w}^h, \mathbf{r}^h_m) + \underline{(\nabla\cdot \mathbf{w}^h, \tau_c \nabla\cdot \mathbf{u}^h)} \quad (24) \\ &(\nabla q^h, \tau_m \mathbf{r}^h_m) \quad (25)\end{aligned}$$

At this point the first, third and last term in the second line of (24) as well as the continuity term in (25) can be identified as the stabilisation terms for the Navier-Stokes equations[22]. They correspond to the case where the negative adjoint Navier-Stokes differential operator is taken for stabilisation purposes, also known as *unusual stabilised finite element method* (USFEM), or *adjoint operator Galerkin least squares stabilisation* (AGLS). Additionally, two nonlinear terms arise which may be interpreted as the missing cross stress and Reynolds stress term. As indicated above, there are several possibilities to approximate the subgrid scale velocity and pressure in Eqs (22) and (23). The simplest has been discussed here and will be used in the numerical examples of the next section.

3.3 Application to a channel flow

In this section, numerical results for the simulation of a turbulent channel flow at $Re_\tau = 180$ are presented, using the approaches described above. The geometrical setup is the same in all cases.

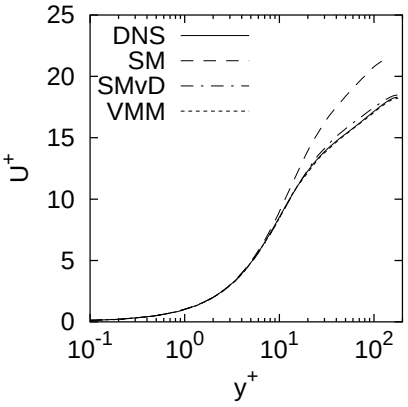

Figure 3: Mean streamwise velocity

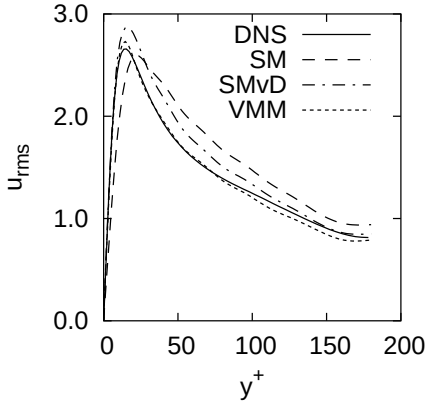

Figure 4: RMS of velocity fluctuation in the streamwise direction

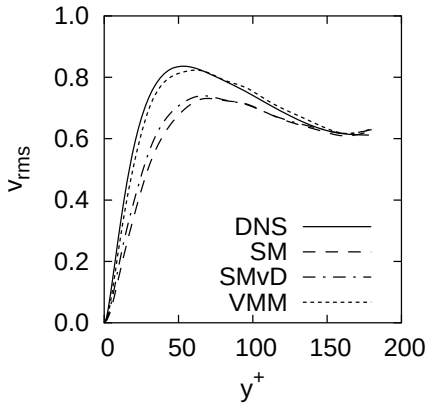

Figure 5: RMS of velocity fluctuation in the wall-normal direction

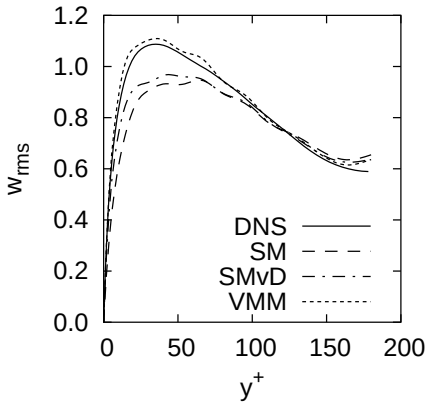

Figure 6: RMS of velocity fluctuation in the spanwise direction

3.3.1 Results for a three-level multiscale method

Results for the three-level VMM were computed with the space-time discretisation for the compressible Navier-Stokes equations. The flow conditions were scaled such that the maximum Mach number was less than 0.3. For the spatial discretisation, a continuous hierarchical basis with linear and quadratic element modes was used on a $16\times16\times16$ mesh. The element geometries were stretched in the wall-normal direction using a hyperbolic tangent function. A discontinuous discretisation was used for the time direction, with linear interpolation and weak enforcement of the initial conditions. The resulting method is third-order accurate in both space and time.

Figure 3 compares the mean streamwise velocity profile from a direct numerical simulation (DNS)[23], computed using a single-scale method (SM), a single-scale method with van Driest damping (SMvD), and a variational multiscale method (VMM). For SM and

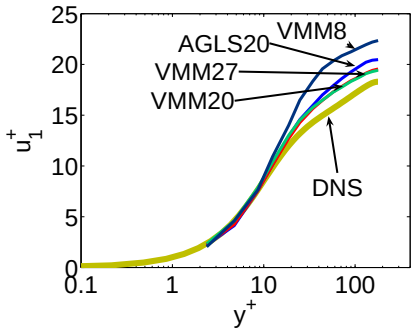

Figure 7: Mean streamwise velocity

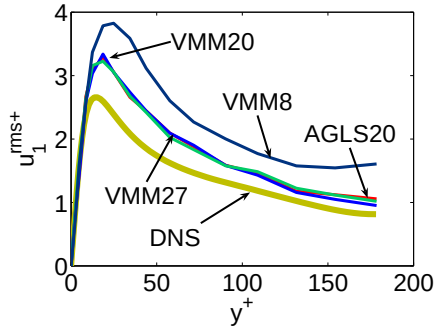

Figure 8: RMS of velocity fluctuation in streamwise direction

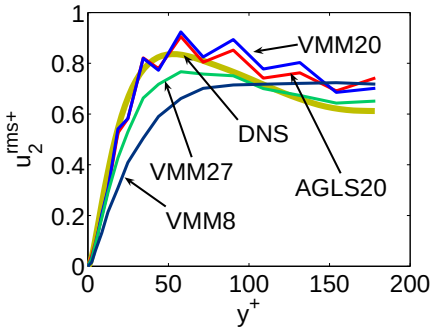

Figure 9: RMS of velocity fluctuation in wall-normal direction

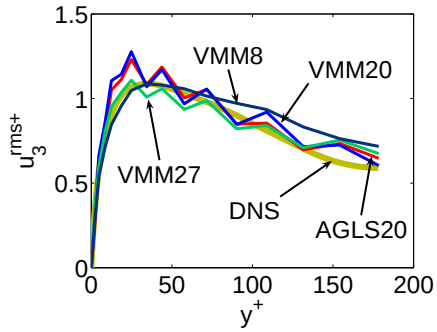

Figure 10: RMS of velocity fluctuation in spanwise direction

SMvD, the unresolved-scale model is applied to all resolved scales, where for the latter case the model coefficient is decreased in magnitude to zero as the wall is approached. In the VMM, a constant-coefficient model is applied only to the resolved scales associated with the quadratic modes. In all cases no additional stabilisation operators were used, in order to limit dissipative mechanisms outside of the viscous and model terms. The SM results for the mean profile differ substantially from those of the DNS. The SMvD results are considerably improved, while the VMM results are virtually indistinguishable from the DNS results.

Figures 4 – 6 compare the RMS velocity profiles for the spatial components of the velocity fluctuations. The VMM results show marked improvement over their SM and SMvD counterparts, in spite of the fact they require slightly less time to compute. Clearly, the wall-normal and spanwise RMS components are attenuated significantly when the dissipative model is applied to the unresolved large scales. This effect is reduced somewhat when the model term is effectively eliminated close to the wall using van Driest damping. In more general cases, a similar effect must be obtained via dynamic modelling in order to achieve acceptable results. The VMM produces good results with a constant-coefficient

model, however, and has in fact been found to be relatively insensitive to the value of the coefficient. This result emphasises the benefit of scale-selective application of the model for unresolved scales.

3.3.2 Residual-based multiscale method

In the residual-based approach a generalised-α time integration is used. The turbulent flow originates from a disturbed laminar flow where the driving force is a constant pressure gradient. In all three spatial directions the channel is discretised by 33 nodes. Hyperbolic tangent mesh stretching is applied in the wall normal direction[24].

Results for three different finite element basis functions and an AGLS-stabilised approach are compared with DNS results[25] in Figures 7 – 10. In these figures VMM8 denotes the residual-based VMM approach using linear basis functions (8-noded hexahedra), while the acronyms VMM20 and VMM27 relate to the results obtained with 20-noded element and with 27-noded elements, respectively. For the AGLS-stabilised approach (AGLS20), a conservative formulation using the 20-noded serendipity element is utilised. This implies that only the underlined terms are used in Eq. (24). This case provides us with a kind of reference solution.

Concerning the computational cost, there is little difference between the residual-based VMM approach and the AGLS approach, since the evaluation of the additional element matrices for the VMM approach is cheap. In contrast, there are significant differences between the cost for linear and quadratic elements. For linear elements, no expensive second derivatives have to be calculated and moreover, the solution of the resulting linear system of equations is cheaper than that of the quadratic elements.

In Figure 7, the normalised mean streamwise velocity u_1^+ is displayed as a function of the wall coordinate y^+. A marked improvement is observed for the quadratic elements AGLS20, VMM20, VMM27 in comparison with the linear elements VMM8. A comparison of the results obtained using VMM8 and AGLS20 shows that elevating the interpolation order has a more significant impact on the accuracy of the results than the inclusion of the VMM model. Focusing on the quadratic elements, this plot shows that the residual-based variational multiscale method yields results that are significantly better results than those obtained with the classical stabilisation approach. These observations carry over to all three spatial directions, see Figures 8 – 10.

4 MULTIGRID METHODS FOR FLUID-STRUCTURE INTERACTION

4.1 From multiscale to multigrid

To elucidate the relation between multiscale and multigrid methods, we consider the canonical variational problem: find $u \in \mathcal{U}$ such that

$$a(u,v) = b(v) \qquad \forall v \in \mathcal{U}, \tag{26}$$

where $\mathcal{U}$ is a certain function space, $a : \mathcal{U} \times \mathcal{U} \to \mathbb{R}$ is a bounded bilinear form and $b : \mathcal{U} \mapsto \mathbb{R}$ is a bounded linear functional. For convenience, we have assumed the trial and test spaces in (26) to be identical. Upon introduction of the partition $\mathcal{U} = \mathcal{U}^h \oplus \hat{\mathcal{U}}$ into complementary coarse and fine-scale subspaces, (26) can be recast into the multiscale form[1,2]: find $(u^h, \hat{u}) \in \mathcal{U}^h \times \hat{\mathcal{U}}$ such that, simultaneously,

$$a(u^h, v^h) + a(\hat{u}, v^h) = b(v^h) \qquad \forall v^h \in \mathcal{U}^h, \tag{27a}$$

$$a(u^h, \hat{v}) + a(\hat{u}, \hat{v}) = b(\hat{v}) \qquad \forall \hat{v} \in \hat{\mathcal{U}}. \tag{27b}$$

It is noted that if the (fine-scale) component $\hat{u} \in \hat{\mathcal{U}}$ is given, the complementary (coarse-scale) component $u^h \in \mathcal{U}^h$ can be extracted from (27a).

Multigrid methods essentially consist of two operations, viz. a smoothing operation and the coarse-grid correction. Denoting by $\Pi : \mathcal{U} \to \mathcal{U}^h$ the orthogonal projection from $\mathcal{U}$ onto $\mathcal{U}^h$, the fine-scale component $\hat{u}$ can be identified as the projection of the actual solution u of (26) onto $\hat{\mathcal{U}}$, i.e., $\hat{u} = u - \Pi u$. The objective of the smoothing operation is to provide an approximation $\tilde{u} \in \mathcal{U}$ such that its projection onto the orthogonal complement, $\tilde{u} - \Pi\tilde{u}$, is close to the projection of the actual solution, $\hat{u}$. Upon replacing $\hat{u}$ in (27a) by the approximation $\tilde{u} - \Pi\tilde{u}$, we obtain the coarse-scale problem: find $\tilde{u}^h \in \mathcal{U}^h$ such that

$$a(\tilde{u}^h, v^h) = a(\Pi\tilde{u}, v^h) + b(v^h) - a(\tilde{u}, v^h) \qquad \forall v^h \in \mathcal{U}^h\,. \tag{28}$$

The approximate coarse-scale solution $\tilde{u}^h$ is in turn used to correct the approximation $\tilde{u} \in \mathcal{U}$ according to $\tilde{u} + \tilde{u}^h - \Pi\tilde{u}$.

To assess the convergence behaviour of the multigrid method, we note that the addition of a suitable partition of zero to the coarse-scale equation (28) yields that the error $\tilde{u} - u$ in the post-smoothing approximation $\tilde{u}$ induces a coarse-scale error $\tilde{u}^h - u^h \in \mathcal{U}^h$ according to

$$a(\tilde{u}^h - u^h, v^h) = -a\big((I - \Pi)(\tilde{u} - u), v^h\big) \qquad \forall v^h \in \mathcal{U}^h\,, \tag{29}$$

which implies that $\|\tilde{u}^h - u^h\|_{\mathcal{U}} \leq \text{const}\,\|(I - \Pi)(\tilde{u} - u)\|_{\mathcal{U}}$. This leads to the following upper bound for the error in the approximation $\tilde{u} + \tilde{u}^h - \Pi\tilde{u}$:

$$\begin{aligned} \big\|(\tilde{u} + \tilde{u} - \Pi\tilde{u}) - u\big\|_{\mathcal{U}} &= \big\|(I - \Pi)(\tilde{u} - u) + (\tilde{u}^h - u^h)\big\|_{\mathcal{U}} \\ &\leq \big\|(I - \Pi)(\tilde{u} - u)\|_{\mathcal{U}} + \|\tilde{u}^h - u^h\big\|_{\mathcal{U}} \\ &\leq \text{const}\,\|(I - \Pi)(\tilde{u} - u)\|_{\mathcal{U}} \end{aligned} \tag{30}$$

Hence, we obtain the fundamental corollary that if the post-smoothing error $\tilde{u} - u$ can be accurately represented in the coarse-scale space and, accordingly, $\|(I - \Pi)(\tilde{u} - u)\|_{\mathcal{U}}$ is sufficiently small, then the multigrid method based on the splitting $\mathcal{U} = \mathcal{U}^h \oplus \hat{\mathcal{U}}$ will exhibit excellent convergence.

The smoother fulfills an essential part in the multigrid process. Further to the conditions on its smoothing properties, the smoother should be feasible and computationally

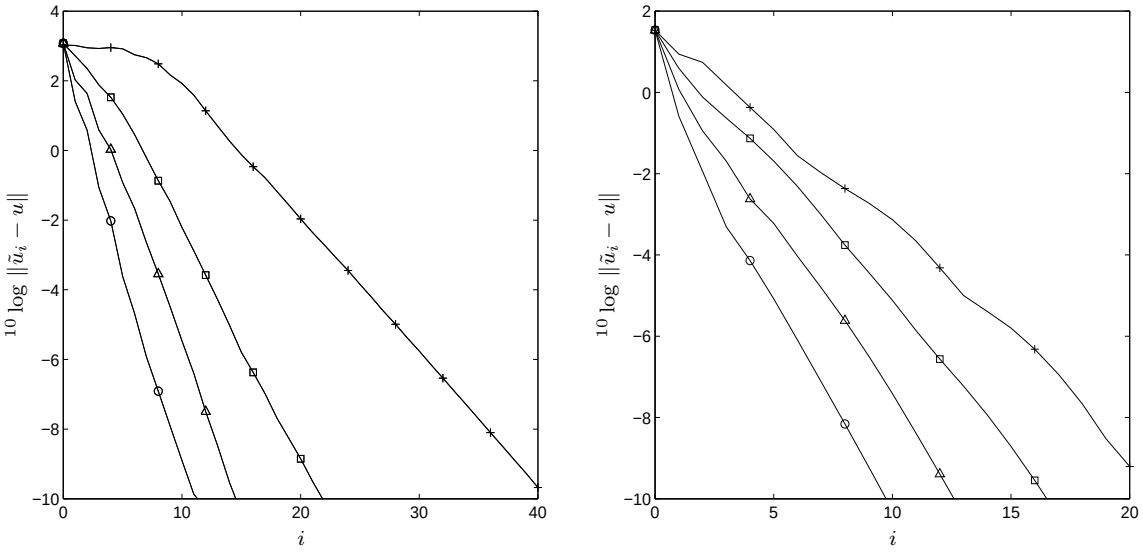

Figure 11: Error $\|\tilde{u}_i - u\|_{\mathcal{U}}$ versus the iteration counter for the sequence of approximations $\{\tilde{u}_i\}$ generated by the two-grid method for a supersonic setting (left) and for a subsonic setting (right), and for $(h,\tau) = 2^{-l}(2^{-2}, 2^{-1})$, $l = 1$ (+), $l = 2$ (□), $l = 3$ (△) and $l = 4$ (○).

inexpensive. In the context of multiscale methods, we note that the right member of (28) represents the effect of the fine scales on the coarse-scale component u^h, provided that $\|(I - \Pi)(\tilde{u} - u)\|_{\mathcal{U}}$ is small. Hence, the smoother in conjunction with the right member of (28) can be conceived as a subgrid-scale model.

4.2 A partitioned smoother for fluid-structure interaction

To apply the above multigrid framework to fluid-structure-interaction problems, we assume that u denotes the displacement of a fluid-structure interface. Moreover, we assume that the underlying operator in (26) admits a splitting of the form $a(u, v) = (v, Su + Pu)$ where the operators S and P indicate a structural and a fluidic part, respectively, so that (26) represents the equilibrium of tractions at the interface[26]. In particular, P represents the so-called *displacement-to-pressure* operator, which associates to each interface-displacement field the pressure that is exerted by the fluid on the structure.

The basic iterative method for solving fluid-structure-interaction problems is *subiteration*. Based on the aforementioned splitting of the operator, the subiteration method is defined by the following *defect-correction process*: given an initial estimate of the interface displacement $u_0 \in \mathcal{U}$,

$$(v, Su_{i+1}) = b(v) - (v, Pu_i) \qquad \forall v \in \mathcal{U} \qquad (i = 0, 1, \ldots)\,. \tag{31}$$

It is to be noted that (31) constitutes a *partitioned* method, as the fluid (P) and structure (S) are treated separately.

In specific cases it can be shown that P is *relatively compact* with respect to S, but this property is believed to be generic for fluid-structure-interaction problems. Loosely speaking, this relative-compactness property implies that the fluid-pressure fields $P\mathcal{U}$ form only a small subspace of the admissible structure-load fields $S\mathcal{U}$. This is connected to the multiscale character of fluid-structure-interaction problems: in general, S is much more sensitive to fine-scale components than P. Conversely, this means that $S^{-1}P$ effectively eliminates fine-scale components. By adding a partition of zero to (31), we obtain the error-amplification relation $(u_{i+1}-u) = -(S^{-1}P)\,(u_i-u)$ and, hence, the defect-correction process (31) yields an excellent smoother. In fact, it can be shown that on sufficiently fine meshes, *one* iteration of (31) supported by a coarse grid-correction (28) renders the error arbitrarily small.

To illustrate the effectiveness of the multigrid process, Figure 11 plots the error reduction obtained by one iteration of (31) followed by a coarse-grid correction from a twice-coarser mesh for the panel problem, for a sequence of increasingly fine meshes[26]. The left and right plots correspond to a subsonic and a supersonic setting, respectively. The results clearly illustrate that indeed the convergence of the method improves as the mesh is refined.

5 CONCLUDING REMARKS

A succinct overview has been given of multiscale methods in computational fluid mechanics and for fluid-structure interaction problems. Some recently developed variational multiscale methods have been briefly elaborated for compressible and for incompressible flows. Results have been shown for application to a channel flow. Finally, multigrid methods have been cast in the format of a multiscale method and their versatility for solving fluid-structure interaction problems has been shown.

REFERENCES

[1] T.J.R. Hughes. Multiscale phenomena: Green's functions, the Dirichlet-to-Neumann formulation, subgrid scale models, bubbles and the origins of stabilized methods. *Comput. Meth. Appl. Mech. Engng.* **127**, 387–401 (1995).

[2] T.J.R. Hughes, G.R. Feijóo, L. Mazzei, and J.B. Quincy. The variational multiscale method – a paradigm for computational mechanics. *Comp. Meth. Appl. Mech. Engng.* **166**, 3–24 (1998).

[3] T.J.R. Hughes, L. Mazzei, K.E. Jansen. Large eddy simulation and the variational multiscale method. *Comput. Visual Sci.* **3**, 47–59 (2000).

[4] T.J.R. Hughes, A.A. Oberai, L. Mazzei. Large eddy simulation of turbulent channel flows by the variational multiscale method. *Physics of Fluids* **13**, 1784–1799 (2001).

[5] A. Brandt. *Multiscale scientific computation: Review 2001.* In T.J. Barth, T.F. Chan, and R. Haimes (eds), *Multiscale and Multiresolution Methods: Theory and Applications*, Springer Verlag, Heidelberg (2001).

[6] W. E and B. Engquist. Multiscale modeling and computation. *Notices of the AMS* **50**, 1062–1070 (2003).

[7] P. Bochev, M. Christon, S.S. Collis, R. Lehoucq, J. Shadid, A. Slepoy, and G. Wagner. A mathematical framework for multiscale science and engineering: The variational multiscale method and interscale transfer operators. *Technical report, Sandia National Laboratories* (2004).

[8] V. Gravemeier. The variational multiscale method for laminar and turbulent flow. *Arch. Comput. Meth. Engng.*, in press.

[9] C. Farhat, I. Harari, and U. Hetmaniuk. The discontinuous enrichment method for multiscale analysis. *Comp. Meth. Appl. Mech. Engng.* **192**, 3195–3209 (2003).

[10] L.P. Franca and A. Nesliturk. On a two-level finite element method for the incompressible Navier-Stokes equations. *Int. J. Numer. Meth. Engng.* **52**, 433–453 (2001).

[11] V. Gravemeier, W.A. Wall, and E. Ramm. A three-level finite element method for the instationary incompressible Navier-Stokes equations. *Comp. Meth. Appl. Mech. Engng.* **193**, 1323–1366 (2004).

[12] V. Gravemeier, W.A. Wall, and E. Ramm. Large eddy simulation of turbulent incompressible flows by a three-level finite element method. *Int. J. Numer. Meth. Fluids* **48**, 1067–1099 (2005).

[13] V.M. Calo. *Residual-based multiscale turbulence modeling: Finite volume simulations of bypass transition.* Ph.D. Thesis, Department of Civil and Environmental Engineering, Stanford University (2005).

[14] S.P. Xiao and T. Belytschko. A bridging domain method for coupling continua with molecular dynamics. *Comp. Meth. Appl. Mech. Engng.* **193**, 1645–1669 (2004).

[15] J. Fish and W. Chen. Discrete-to-continuum bridging based on multigrid principles. *Comp. Meth. Appl. Mech. Engng.* **193**, 1693–1711 (2004).

[16] K.E. Jansen, A.E. Tejada-Martínez. An evaluation of the variational multiscale method for large-eddy simulation while using a hierarchical basis. *AIAA paper* 2002-0283 (2002).

[17] S.S. Collis. The DG/VMS method for unified turbulence simulation. *AIAA paper* 2002-3124 (2002).

[18] B. Koobus, C. Farhat. A variational multiscale method for the large eddy simulation of compressible turbulent flows on unstructured meshes – application to vortex shedding. *Comp. Meth. Appl. Mech. Engng.* **193**, 1367–1383 (2004).

[19] E. Munts. *Space-Time Multiscale Methods for Large-Eddy Simulation.* Dissertation, Delft University of Technology (2006).

[20] D.K. Lilly. *The length scale for subgrid-scale parameterization with anisotropic resolution.* CTR Annual Research Briefs, 3–9. Stanford University/NASA Ames Research Center (1988).

[21] T.J.R. Hughes, G. Sangalli. Variational multiscale analysis: the fine-scale Green's function, projection, optimization, localization, and stabilized methods. *Technical Report 05-46, ICES, University of Texas, Austin*, http://www.ices.utexas.edu/research/reports/2005.php (2005).

[22] T.J.R. Hughes, G. Scovazzi, L. Franca. *Encyclopedia of Computational Mechanics*, Vol. 3, Wiley, Chichester (2004).

[23] P. Moin, J. Kim. Numerical investigation of turbulent channel flow. *J. Fluid Mechanics*, **118** 341–371 (1982).

[24] S. Lenz, W.A. Wall. A residual-based variational multiscale method and its application to incompressible turbulent channel flow. *Theor. Comp. Fluid Dyn.*, submitted.

[25] J. Kim, P. Moin, R. Moser. Turbulence statistics in fully developed channel flow at low reynolds number. *J. Fluid Mechnics* **177**, 133–166 (1987)

[26] E.H. van Brummelen, K.G. van der Zee, R. de Borst. *Space/time multigrid for a fluid-structure-interaction problem*, Delft Aerospace Computational Science Report DACS-06-004, http://www.em.lr.tudelft.nl/downloads/DACS-06-004.pdf (2006).